DOI: 10.1002/((please add manuscript number))
Article type: Communication

Metamaterial analogue of Ising model

*Longqing Cong, Vassili Savinov, Yogesh Kumar Srivastava, Song Han, and Ranjan Singh**

Dr. Longqing Cong, Yogesh Kumar Srivastava, Song Han, and Prof. Ranjan Singh
Division of Physics and Applied Physics, School of Physical and Mathematical Sciences, Nanyang Technological University, Singapore 637371, Singapore
Centre for Disruptive Photonic Technologies, The Photonics Institute, Nanyang Technological University, 50 Nanyang Avenue, Singapore 639798, Singapore
*E-mail: ranjans@ntu.edu.sg
Dr. Vassili Savinov
Optoelectronics Research Centre and Centre for Photonic Metamaterials, University of Southampton, Southampton, SO171BJ, United Kingdom

Keywords: metamaterials, Ising model, terahertz, Fano

Abstract: The interaction between microscopic particles has always been a fascinating and intriguing area of science. Direct interrogation of such interactions is often difficult. Structured electromagnetic systems offer a rich toolkit for mimicking and reproducing the key dynamics that governs the microscopic interactions, and thus provide an avenue to explore and interpret the microscopic phenomena. In particular, metamaterials offer the freedom to artificially tailor light-matter coupling and to control the interaction between unit cells in the metamaterial array. Here we demonstrate a terahertz metamaterial that mimics spin-related interactions of microscopic particles in a 2D lattice via complex electromagnetic multipoles scattered within the metamaterial array. Fano resonances featured by distinct mode properties due to strong nearest-neighbor interactions are discussed that draw parallels with the 2D Ising model. Interestingly, a phase transition from single Fano resonance to hyperfine splitting of Fano spectrum is observed by manipulating

the 2D interactions without applying external magnetic or electric fields, which provides a potential multispectral platform for applications in super-resolution imaging, biosensing, and selective thermal emission. The dynamic approach to reproduce static interaction between microscopic particles would enable more profound significance in exploring the unknown physical world by the macroscopic analogues.

Interaction between large aggregates of particles lies at the heart of our understanding of complex macroscopic behaviors exhibited by solids, gases, and fluids near phase transitions.[1] Models of particle interactions provide a framework for study and classification of critical phenomena, and are thus important in modelling a wide variety of scenarios ranging from solid state physics to high-energy physics, biology of complex systems, and even economics.[2] One of the simplest models that captures a significant share of dynamics of this kind is the two-dimensional (2D) Ising model[3]: a 2D lattice of particles which have a 'spin', i.e. a magnetic dipole moment. The energy of this system depends on the orientation of different spins relative to each other as well as relative to an externally applied magnetic field. The analytical description of the basic 2D Ising model has been available since 1944,[4] but the model remains of interest both in the context of understanding properties of Ising models in higher dimensions, as well as describing 2D Ising-like systems with complex interactions that are not captured by the analytical description. In this work we show how metamaterials, a class of man-made electromagnetic media, can be used to mimic and therefore experimentally explore the properties of 2D Ising model.

Metamaterials are artificial media created by patterning unit cells on the scale smaller than the target wavelength of the electromagnetic excitation.[5] Here we investigate metamaterials composed of terahertz asymmetric split ring resonators (TASR) housed on a low-loss dielectric substrate, as shown in **Figure 1a**. Each TASR is a metallic square with split gaps at the top and bottom sides. The top split is displaced horizontally from the vertical line of symmetry of TASR by distance *d*, therefore, the TASR is split into two

metallic segments of different length. Due to asymmetry in segment length, incident light at normal direction polarized along the metallic segments (*y*-axis in Figure 1a) can excite anti-symmetric current oscillations in the two segments. It is clearly known that in a symmetric split ring resonator (SRR), a broad dipole resonance would be excited with the incident wave polarized along the symmetric axis of the resonator. An inherently nonradiative mode under symmetric SRR becomes weakly radiative when symmetry is broken so that it interferes with the background dipole mode resulting in the observable trapped mode resonance[6, 7] as well as Fano resonance in the spectra.[8, 9] At the Fano resonance, the anti-symmetric current oscillations minimize the energy lost to free space, resulting in a narrow resonance mode.[6]

All the discussion in this work will center on the response of TASR metamaterials at the Fano resonance, and in particular on interactions between the individual TASRs. We therefore introduce a convenient model of a single TASR operating at the trapped mode, as shown in Figure 1b, which represents it as two electric dipoles and one magnetic dipole. As discussed above, the Fano resonance corresponds to opposing current oscillations in the two metallic segments of each TASR, which would give rise to an out-of-plane magnetic dipole (M_z). In an asymmetric meta-atom, such as considered here, the Fano mode also corresponds to electric dipoles along *y*-axis (P_y) as well as *x*-axis (P_x), which arise due to lack of mirror symmetry in vertical and horizontal axis. An important property of TASR metamaterials, at the Fano resonance, is that strong magnetic-dipole-mediated interactions between the neighboring TASRs lead to emergence of the so-called collective mode or cooperative resonance,[10, 11] where the whole metamaterial behaves as a single planar

cavity (see Figure 1a). In this work, we will demonstrate the direct analogy between the interactions of dynamic dipoles in TASR metamaterials and the interactions of static dipoles, which are important in Ising model, as well as in shaping magnetic and electric ordering in ferromagnetic and ferroelectric materials.[12]

Our analysis will focus on two kinds of TASRs, which are mirror images of each other and defined according to the positions of top split gap as '*left*' and '*right*'. In all cases the metamaterial will be driven by vertically polarized radiation (along *y*-axis in Figure 1a) at normal incidence. Therefore, the vertical electric dipole induced in the '*left*' and '*right*' TASRs will be identical in the two kinds of resonators, but the orientation of accompanying horizontal electric dipole and out-of-plane magnetic dipole will be reversed as illustrated in Figure 1c. The link between the geometry of the TASRs and the orientation of electric (P_x) and magnetic dipoles (M_z) induced in them allows building complex multipole excitations out of individual TASR, and investigating Ising model interactions. For example, a combination of a '*left*' and '*right*' TASR loops, as shown in Figure 1d, corresponds to *xy*-electric quadrupole, and a superposition of toroidal dipole and magnetic quadrupole.

We begin by considering four metamaterials with composite periodic supercells (S_1, S_2, S_3, S_4) that consist of four TASRs in square lattice arrangement (left column of **Figure 2**). We note that the interactions discussed in this work are not limited to one supercell, but applied to the whole metamaterial array that is comprised of ~4000 supercells (infinite in simulations). S_1 consists exclusively of *right* TASRs, whereas the other three types of

supercells represent all possible permutations in which two out of four TASRs in each supercell are '*right*' and the other two are '*left*'. The left column in Figure 2 denotes the relative orientation of the magnetic dipoles of the four TASRs at one oscillation phase of Fano resonance (for S_1 all magnetic dipoles point up). Drawing parallel with magnetic materials, we note that metamaterial S_1 can be regarded as a representation of a ferromagnetic material, with magnetic dipoles of all domains (TASRs) pointing in the same direction, whilst the other three metamaterials (S_2-S_4) correspond to antiferromagnetic materials. Furthermore, as shown in Figures 1b and 1c, single TASR corresponds to both horizontal electric and out-of-plane magnetic dipoles. The metamaterials S_1-S_4 are therefore metamaterial analogues of multiferroic materials.[12]

The strong interactions between the unit cells (nearest-neighbor interaction) in TASR metamaterials[13] make it virtually impossible to use the hybridization approach[14] to explain how complex TASR metamaterial response arises out of dispersion properties of individual metallic segments. Instead, we analyze the resonant response based on interaction energy. The dynamics of each charged particle in the metamaterial is governed by the Lagrangian $L = L_k - \int d^3 r \left(\rho\phi - \vec{A} \cdot \vec{J} \right)$ [15], where L_k is the kinetic part of the Lagrangian, ρ, $\vec{J}$ are charge and current density due to particles, and ϕ, $\vec{A}$ are scalar and vector potentials. The above Lagrangian is a general modality, and we simplify it by assuming that (1) response of each individual TASR in the metamaterial, when driven near the resonant frequency, is well-approximated by a simple harmonic oscillator with resonant angular frequency ω_0; (2) metamaterial is driven by plane wave at normal incidence. So the excitation of all unit cells can be described by a single dynamic variable $X = X(t)$

(ignoring the edge effects). The Lagrangian then becomes:

$$L = \frac{1}{2}\dot{X}^2 - \frac{\omega_0^{\,2}}{2}X^2 - \int_{inter-resonator} d^3r\left(\rho\phi - \vec{A}\cdot\vec{J}\right) \quad (1)$$

The first part of the Largangian ensures response of a simple harmonic oscillator with angular frequency ω_0, and the second part of the Lagrangian couples the metamaterial to incident radiation as well as taking into account interactions between the constituent unit cells of the metamaterial.

As illustrated in Figure 1, each TASR of the metamaterial, at Fano resonance can be approximated as electric and magnetic dipoles. Associating the variable $X(t)$ with induced charge density, it is possible to show that the resonant frequency of the whole metamaterial will be given by (see supporting information Note 2)

$$\Omega = \sqrt{\frac{\omega_0^{\,2} + \alpha}{1 - \gamma/\omega_0^{\,2}}} + \Omega_{near} \approx \omega_0 + \frac{\alpha + \gamma}{2\omega_0} + \Omega_{near} \quad (2)$$

where α is related to electric dipole-dipole interaction energy and γ is related to magnetic dipole-dipole interaction energy between the TASRs. An additional frequency shift Ω_{near} is added to account for the left-over high-order multipole interactions between the nearest-neighbor TASRs. One can now draw direct parallels with the Ising model: The energy of the system is mimicked by the resonant frequency Ω, and Ω_{near} mimics the exchange interactions between the neighboring unit cells, whilst $\frac{\alpha+\gamma}{2\omega_0}$ describes the long-range dipole-dipole interactions. Thus one obtains a correspondence between the interaction energy considered in the case of static Ising models, and the resonant frequency shift observed in dynamic TASRs and other metamaterial systems.

In order to verify the understanding, four sets of metamaterials S_1-S_4 were designed, fabricated by standard photolithography, and characterized using an antenna based terahertz time-domain spectroscopy system (THz-TDS; see supporting information Note 4). Additionally, the response of the four metamaterials was also modelled on a numerical solver (CST Microwave Studio). The measured and computed transmission intensity spectra of the four metamaterials are obtained from $T(\omega)=\left(\tilde{t}_s(\omega)/\tilde{t}_r(\omega)\right)^2$ as shown in the central column of Figure 2, where $\tilde{t}_s(\omega)$ and $\tilde{t}_r(\omega)$ are the transmission amplitude of samples and reference (silicon substrate in dry nitrogen atmosphere) after Fourier transform, respectively. In time-domain measurements, a scan time of 200 ps was carried out giving rise to a ~5 GHz frequency resolution in order to capture the sharp spectral features. Each transmission spectrum was obtained by averaging 1000 scans in real time to ensure the accuracy of measured data. We first focus our attention on the spectral position of the metamaterial transmission dips, and it is visualized that there is a resonance frequency deviation from S_1 to S_4 for the Fano resonance in experiments as well as in simulations. Different supercell configurations enable various nearest-neighbor interactions which dominate the collective resonance frequency at the Fano mode. The corresponding resonances occur at frequencies $\Omega_1/2\pi=0.52$ THz, $\Omega_2/2\pi=0.50$ THz, $\Omega_3/2\pi=0.48$ THz, and $\Omega_4/2\pi=0.44$ THz, for metamaterials S_1-S_4 in experiments, respectively. The measured frequency shift exactly follows the trend of simulations (see supporting information Note 4).

The four metamaterials in Figure 2 present a perfect test-bed for the investigation of the

interactions that govern the dynamics of TASR and similar metamaterials. For example, the comparison shows that dipole-dipole interaction energy (see supporting information Note 5) of the S_2 metamaterial (Figure 2b) is lower than that of S_4 (Figure 2d) metamaterial, yet the resonant frequency of S_2 is higher than that of S_4. Equation 2 therefore suggests that resonant frequency shift, and thus the nearest-neighbor unit cell interactions are dominated by near-field terms (related to higher order multipoles, Ω_{near}) rather than by dipole-dipole interactions as is commonly assumed in case of asymmetric split ring metamaterials (see supporting information Note 9 for quantitative comparison).[9, 10, 11] Here, the analogy between the TASR metamaterial driven at Fano resonance and the Ising model is established through the formalism of Hamiltonian. The interaction of the Hamiltonian[16] for the Ising model is described by

$$H_{Is} = -\sum_{i=1}^{N} B\mu s_i - J\sum_{*i,j}^{N} s_i s_j$$

where sums run over N particles, B is the applied magnetic field, $s_i = \pm 1/2$ is projection of the spin along the z-axis, μ is the magnetic dipole moment of a particle and J is the coupling parameter that encodes the energy between neighboring particles. The '$*$' in the second sum denotes that it sums interactions of the nearest neighbors only. For TASR metamaterial system, the Hamiltonian is described with some standard manipulations, which maps directly into the standard Ising model. The incident radiation now takes the role of the applied magnetic field in the original Ising model. This analogy can be extended further by introducing equivalents of *microstates*, *order parameter*, *entropy*, *thermodynamic energy*, and even '*temperature*' for the TASR metamaterial (see supporting information Note 8).

The dominant role of the strong nearest-neighbor interaction also reflects on the tailoring of far-field radiation multipoles via deploying the multipoles in different metamaterial configurations, which results in the reconfiguration of resonance quality factors. As presented in Figure 1d, the resultant multipoles at the Fano resonance are tailored by the strong interaction between resonators, which would enable the manipulation of radiative properties of the Fano mode. The respective multipole analysis (see supporting information Note 1) is performed for the four cases with distinct magnetic and electric dipole interactions as shown in the third column of Figure 2. Consistent with Figure 1b for S_1 with identical resonators, the electric dipole along *y*-axis (P_y) dominates the scattering, together with a magnetic dipole along *z*-axis (M_z). In this coherent resonance, the electric dipole has been largely suppressed which thus results in a low-loss Fano resonance characterized by the quality factor (Q, Q = 11.8). A higher order mode, electric quadrupole (Q^e), appears as a result of superposition of electric dipole along *x* axis (P_x).

As for S_2, a pair of anti-aligned magnetic dipoles, created by two co-planar current loops, corresponds to a superposition of a toroidal dipole[17] and a magnetic quadrupole. It has also been shown that in case of planar metamaterials the substrate can act as an additional magnetic dipole, making the combination of two co-planar currents *on* the substrate, to respond predominantly as an in-plane toroidal dipole.[18] The two pairs of anti-aligned magnetic dipoles in supercell S_2 therefore add up to a net toroidal dipole along the *x*-axis (T_x). It is verified from the multipole analysis where the suppression of M_z and enhancement of T_x accompanied with Q^m are visualized. Note that electric dipole scattering far exceeds the scattering rate of all the other multipoles, and the toroidal dipole is

orthogonal to electric dipole. The additional scattering through toroidal dipole and magnetic quadrupole therefore have negligible effect on radiation loss, hence the *Q* factor of S_2 is almost the same as that of S_1.

As illustrated in Figure 2c for S_3, the configuration of magnetic dipoles in the supercell is such that it gives rise to two pairs of toroidal dipoles at resonance. One pair is aligned along the *y*-axis, whilst the other lies along the *x*-axis. In both pairs the two individual toroidal dipoles oscillate in anti-phase, leading to net suppression of toroidal dipole both along the *x*- and the *y*-axis. This analysis is supported by the drop in the scattered power of toroidal dipole at resonance (see analysis in Figure 2c). The resultant experimental and simulated transmission spectra show that the *Q* factor is slightly increased (Q = 12.0 in experiment). The scattered power of multipoles also confirms that all the multipoles except electric dipole are suppressed which effectively reduces the radiative losses from these higher order multipoles, and thus resulting in the slightly increased *Q* factor of Fano resonance.

A more interesting scenario exists in S_4, where the toroidal dipole along *y* axis (T_y) is enhanced. This toroidal dipole has the same orientation as the dominant electrical dipole so that interference will occur between them. A destructive interference (T_y and P_y oscillate anti-phase, see supporting information Note 3) effectively reduces the radiative loss, enabling a much improved *Q* factor of the resultant Fano resonance (Q = 23.1 in simulation, and Q = 15.1 in experiment) as shown in Figure 2d. Such an in-plane toroidal dipole parallel to the electric dipole could be tailored for a nonradiative anapole configuration by tuning their intensity and phase for a completely destructive interference.[19] Here the noticeable

difference of quality factor originates from experiment limitations, such as fabrication defects, roughness of sample surface, and dispersion in constituent materials (see supporting information Note 7).

By mimicking the dynamic dipoles in metamaterial to an Ising model, we have investigated the effects of nearest-neighbor interactions on Fano resonance in terms of the resonant energy as well as the quality factor where higher order multipoles (including toroidal dipole) play a dominant role. All the four Fano resonances under the respective multipole configurations reveal distinct properties that could behave as the topological eigen modes of the respective scenarios. Benefitting from the design flexibility of metamaterials, a more complex scenario is probed under the Ising model analogy, where a "*phase transition*" was observed from a single mode Fano spectrum to a hyperfine mode splitting spectrum in absence of external static magnetic/electric field analogous to the Zeeman/Stark effects. As the inset image shown in **Figure 3a** for supercell S_5 with only one resonator mirrored, the measured transmission spectrum shows four separated dips that correspond to the Fano modes supported by supercells S_1, S_2, S_3 and S_4, respectively. Such a hyperfine mode splitting spectrum is clearly captured in simulations as shown in Figure 3b, where the resonance dips coincide with the respective Fano modes of supercells S_1, S_2, S_3 and S_4. We note that the simulated spectral resolution is better than the experimental spectrum which originates from the overall lower quality factors of Fano resonances in experiments (see supporting information Note 7).[11, 20]

The dominant role of nearest-neighbor interaction between unit cells is clearly revealed in

the asymmetric supercell S_5 where all the possible interaction channels in a 2×2 supercell are activated simultaneously. Different electric and magnetic dipole distributions are resumed at the four resonance frequencies as indicated in Figure 3c, that correspond to various multipole configurations. In addition to the first part of the Largangian that originates from the individual harmonic oscillator (ω_0), nearest-neighbor interaction under the Ising model analogue provides an extra freedom to engineer the mode properties through manipulating the spatial topology, and more promising phenomena could be predicted for higher order supercell arrangement as well as three-dimensional configuration.

The faint spectral features of S_5 enables the difficulty in capturing the spectral features that is due to the low density of the mirrored resonators.[20, 21] One solution is by tailoring the gap displacement (d). The larger displacement of the gap would give rise to a stronger coupling of electric dipole to free space in the collectively oscillating mode, and thus result in a more pronounced spectral feature (see supporting information Note 6).[22] The flexibility of metamaterials also reflects on the scalability of operation bands into infrared and visible regimes via tailoring the geometric size of unit cells, and the hyperfine mode splitting spectrum could be adopted in a plethora of fields including biosensing,[23] imaging,[24] and selective thermal emitter.[25] Since Fano resonance has been demonstrated as an excellent platform for refractometric sensing,[23, 26] we summarized the spectral properties of four individual Fano modes in terms of sensitivity in **Table 1**. We note that each mode reveals exclusive sensitivity and spectral quality factor mediated by various multipoles, which provides multispectral fingerprints and resolutions.

In conclusion, we have investigated a metamaterial analogy of static Ising model mediated by the multipoles of Fano resonance. Strong nearest-neighbor interactions in a 2D metamaterial array dominate the collective resonance energy as well as mode quality factors. A hyperfine mode splitting Fano spectrum is observed in the absence of external magnetic/electric field due to simultaneous activation of all the interaction configurations, that provides a flexible path for multispectral excitation and broadband applications. A finer mode splitting spectrum is expected at a higher order supercell (3×3, 4×4, *et al*), which would enable an excellent platform for ultrasensitive sensing, super-resolution imaging, and multiband selective thermal emission. This work also demonstrates a potential path towards investigation of static interactions between microscopic particles by using the macroscopic artificial electromagnetic resonators.

Supporting Information
Supporting Information is available from the Wiley Online Library or from the author.

Acknowledgements

The authors acknowledge research funding support from Singapore Ministry of Education (Grants No. MOE2016-T3-1-006(S) and MOE2017-T2-1-110), Singapore National Research Foundation (NRF) and the French National Research Agency (ANR) (Grant No. NRF2016-NRF-ANR004), and UK's Engineering and Physical Sciences Research Council (Grant Nos. EP/G060363/1 and EP/M009122/1).

Conflict of Interest

The authors declare no conflict of interest.

Received: ((will be filled in by the editorial staff))
Revised: ((will be filled in by the editorial staff))
Published online: ((will be filled in by the editorial staff))

References:

[1] K. De'Bell, A. B. MacIsaac, J. P. Whitehead, *Rev. Mod. Phys.* **2000**, *72*, 225.
[2] A. Pelissetto, E. Vicari, *Phys. Rep.* **2002**, *368*, 549.
[3] D. Chandler, *Introduction to Modern Statistical Mechanics*, Oxford University Press, NY, USA **1987**.
[4] L. Onsager, *Phys. Rev.* **1944**, *65*, 117.
[5] a) N. I. Zheludev, Y. S. Kivshar, *Nat. Mater.* **2012**, *11*, 917; b) D. R. Smith, J. B. Pendry, M. C. Wiltshire, *Science* **2004**, *305*, 788.
[6] V. Fedotov, M. Rose, S. Prosvirnin, N. Papasimakis, N. Zheludev, *Phys. Rev. Lett.* **2007**, *99*, 147401.
[7] a) S. Yang, Z. Liu, X. Xia, Y. E, C. Tang, Y. Wang, J. Li, L. Wang, C. Gu, *Phys. Rev. B* **2016**, *93*, 235407; b) S. Yang, C. Tang, Z. Liu, B. Wang, C. Wang, J. Li, L. Wang, C. Gu, *Opt. Express* **2017**, *25*, 15938.
[8] a) B. Luk'yanchuk, N. I. Zheludev, S. A. Maier, N. J. Halas, P. Nordlander, H. Giessen, C. T. Chong, *Nat. Mater.* **2010**, *9*, 707; b) B. Norman, A. N. Ibraheem, J. Christian, S. Ranjan, M. J. V., S. Maik, K. Martin, *Adv. Opt. Mater.* **2015**, *3*, 642.
[9] a) V. Fedotov, A. Tsiatmas, J. Shi, R. Buckingham, P. De Groot, Y. Chen, S. Wang, N. Zheludev, *Opt. Express* **2010**, *18*, 9015; b) R. Singh, I. A. I. Al-Naib, M. Koch, W. Zhang, *Opt. Express* **2011**, *19*, 6312.
[10] a) S. D. Jenkins, J. Ruostekoski, *Phys. Rev. B* **2012**, *86*, 205128; b) S. D. Jenkins, J. Ruostekoski, *Phys. Rev. B* **2012**, *86*, 085116; c) D. J. Stewart, R. Janne, *New J. Phys.* **2012**, *14*, 103003.
[11] V. A. Fedotov, N. Papasimakis, E. Plum, A. Bitzer, M. Walther, P. Kuo, D. P. Tsai, N. I. Zheludev, *Phys. Rev. Lett.* **2010**, *104*, 223901.
[12] N. A. Spaldin, *Magnetic materials: fundamentals and applications*, Cambridge University Press, NY, USA **2010**.
[13] V. Savinov, V. A. Fedotov, P. A. de Groot, N. I. Zheludev, *Supercon. Sci. Technol.* **2013**, *26*, 084001.
[14] P. Nordlander, C. Oubre, E. Prodan, K. Li, M. Stockman, *Nano Lett.* **2004**, *4*, 899.
[15] L. D. Landau, E. M. Lifshitz, *Course of theoretical physics*, Elsevier, Oxford, UK 2013.
[16] D. V. Schroeder, *An Introduction to Thermal Physics*, Addison Wesley, San Francisco, CA, USA **2000**.
[17] a) T. Kaelberer, V. A. Fedotov, N. Papasimakis, D. P. Tsai, N. I. Zheludev, *Science* **2010**, *330*, 1510; b) Y. Fan, Z. Wei, H. Li, H. Chen, C. M. Soukoulis, *Phys. Rev. B* **2013**, *87*, 115417; c) Z.-G. Dong, J. Zhu, J. Rho, J.-Q. Li, C. Lu, X. Yin, X. Zhang, *Appl. Phys. Lett.* **2012**, *101*, 144105; d) Z.-G. Dong, P. Ni, J. Zhu, X. Yin, X. Zhang, *Opt. Express* **2012**, *20*, 13065.
[18] a) M. Gupta, V. Savinov, N. Xu, L. Cong, G. Dayal, S. Wang, W. Zhang, N. I. Zheludev, R. Singh, *Adv. Mater.* **2016**, *28*, 8206; b) S. Yang, Z. Liu, L. Jin, W. Li, S. Zhang, J. Li, C. Gu, *ACS Photonics* **2017**, *4*, 2650; c) L. Cong, Y. K. Srivastava, R. Singh, *Appl. Phys. Lett.* **2017**, *111*, 081108.
[19] A. E. Miroshnichenko, A. B. Evlyukhin, Y. F. Yu, R. M. Bakker, A. Chipouline, A. I. Kuznetsov, B. Luk'yanchuk, B. N. Chichkov, Y. S. Kivshar, *Nat. Commun.* **2015**, *6*, 8069.
[20] R. Singh, C. Rockstuhl, W. Zhang, *Appl. Phys. Lett.* **2010**, *97*, 241108.

[21] Y. Yang, Kravchenko, II, D. P. Briggs, J. Valentine, *Nat. Commun.* **2014**, *5*, 5753.
[22] L. Cong, M. Manjappa, N. Xu, I. Al-Naib, W. Zhang, R. Singh, *Adv. Opt. Mater.* **2015**, *3*, 1537.
[23] C. Wu, A. B. Khanikaev, R. Adato, N. Arju, A. A. Yanik, H. Altug, G. Shvets, *Nat. Mater.* **2012**, *11*, 69.
[24] Y. Hiraoka, T. Shimi, T. Haraguchi, *Cell Struct. Funct.* **2002**, *27*, 367.
[25] X. Liu, T. Tyler, T. Starr, A. F. Starr, N. M. Jokerst, W. J. Padilla, *Phys. Rev. Lett.* **2011**, *107*, 045901.
[26] R. Singh, W. Cao, I. Al-Naib, L. Cong, W. Withayachumnankul, W. Zhang, *Appl. Phys. Lett.* **2014**, *105*, 171101.

Table 1. Spectral properties of four individual Fano modes

	S_1	S_2	S_3	S_4
Frequency (THz)	0.49	0.47	0.46	0.42
Sensitivity[a] (GHz/RIU)	45.5	41.3	39.6	37.5
***Q* factor**	13.9	13.6	14.7	23.7

[a]Sensitivity is for refractometric sensing with 20 μm thick analyte on top of metasurface in simulations.

Figure captions:

Figure 1. Complex multipole excitations in terahertz asymmetric split ring metamaterials at Fano resonance. (a) Artistic impression of the TASR metamaterial with surface currents. (b) Simplified multipole representation of a single TASR. Black curved arrows denote opposing currents that oscillate in the two metallic segments of the ring. The ring can be represented as a superposition of two electric dipoles (P_x and P_y) and a magnetic dipole (M_z). (c) Multipole representation of the left- and right-oriented split ring driven by vertically polarized radiation at normal incidence. The orientation of driving radiation constrains the vertical electric dipole to be the same in both cases, but the orientations of horizontal electric dipole (P_x) as well as magnetic dipole (M_z) change. (d) Multipole decomposition of a supercell consisting of left and right TASRs, illustrating how individual rings can be combined to create complex excitations accessible with normal incident plane wave.

Figure 2. Metamaterial analogues of multiferroic materials. Left column: (a) One supercell (S_1) with four identical '*right*' TASRs. The four TASRs are evenly distributed in the 160×160 μm lattice. The TASR is made of aluminum with wire width 6 μm, length 60 μm, thickness 0.2 μm and gap width 3 μm. The asymmetry is obtained by displacing the top gap with distance d = 10 μm. (b-d) Supercells S_2-S_4 obtained by mirroring two out of four TASRs in S_1 around the vertical axis. The bull's eye (⊙) and crossed circle (⊗) pictograms in S_2-S_4 denote the orientation of magnetic dipole in the TASR loops at Fano resonance. Alongside out-of-plane magnetic dipoles, the loops will also correspond to electric dipoles as illustrated in Figure 1. **Central column:** Measured and modelled

transmission spectra of the metamaterials with annotated quality factor (Q) of the Fano transmission dip. **Right Column:** Multipole representation of each supercell in the vicinity of Fano mode.

Figure 3. Scenario of asymmetric supercell S_5. (a), (b) Experimental and simulated transmission spectra of S_5 with Fano spectra of S_1, S_2, S_3 and S_4 as background for comparison, respectively. Only one resonator is mirrored in supercell S_5. (c) Schematic current distributions for S_5 at the four different resonance frequencies, which enable the same multipole configurations as that of S_1 to S_4.

Figure. 1

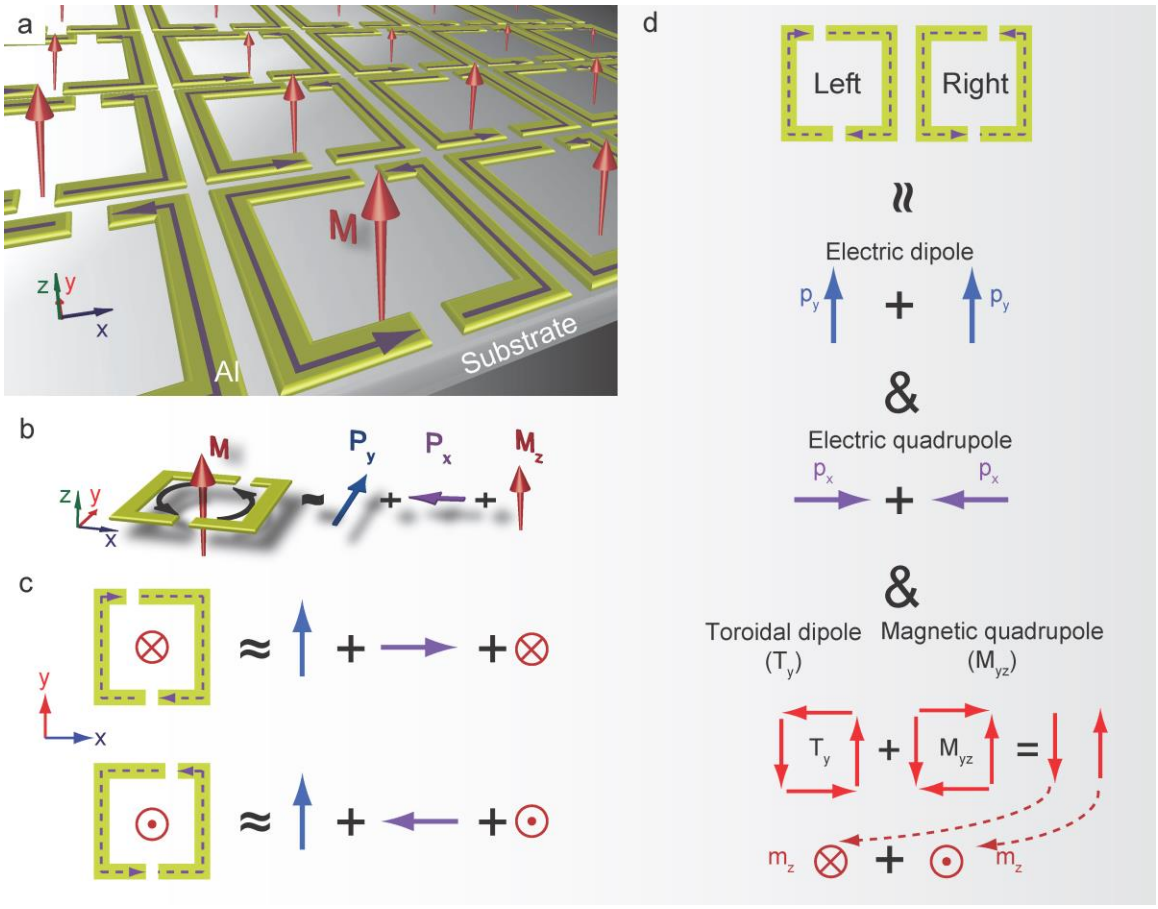
a
M
z
y
x
Al
Substrate
b
M
P_y
P_x
M_z
z
y
x
c
y
x
d
Left
Right
Electric dipole
p_y
p_y
Electric quadrupole
p_x
p_x
Toroidal dipole (T_y)
Magnetic quadrupole (M_{yz})
T_y
M_{yz}
m_z
m_z

Figure. 2

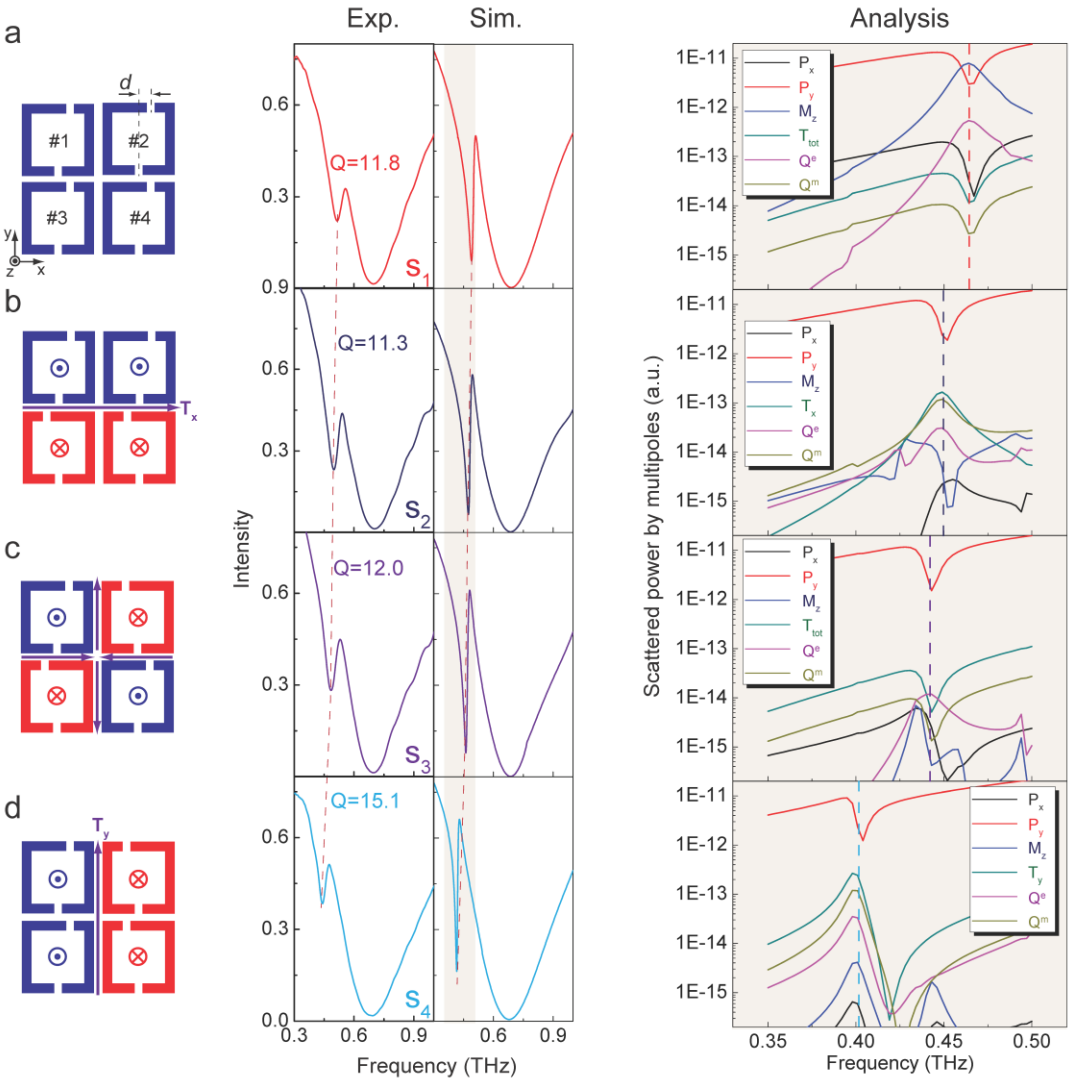
a
b
c
d
d
#1
#2
#3
#4
y
z
x
T_x
T_y
Exp.
Sim.
Analysis
Q=11.8
Q=11.3
Q=12.0
Q=15.1
S_1
S_2
S_3
S_4
Intensity
Scattered power by multipoles (a.u.)
Frequency (THz)
Frequency (THz)
P_x
P_y
M_z
T_{tot}
T_x
T_y
Q^e
Q^m

Figure. 3

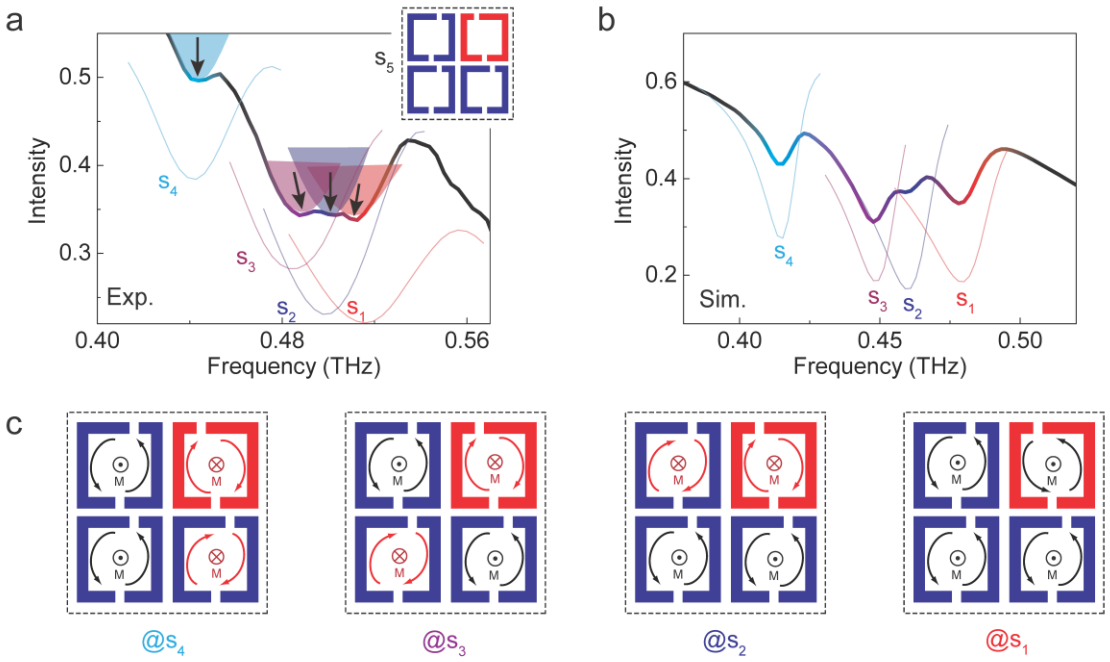
a
Intensity
0.5
0.4
0.3
Exp.
s5
s4
s3
s2
s1
0.40
0.48
0.56
Frequency (THz)
b
Intensity
0.6
0.4
0.2
Sim.
s4
s3
s2
s1
0.40
0.45
0.50
Frequency (THz)
c
M
@s4
@s3
@s2
@s1

Table of contents

2D Ising model of microscopic particles is mimicked via macroscopic subwavelength metamaterial cavities. A hyperfine mode splitting is experimentally demonstrated via manipulation of dynamic multipole interactions in the absence of external electric/magnetic field, which not only enriches the understanding of spin-related interactions in Ising model, but also holds tremendous significance in subwavelength photonic applications such as sensing and hyperspectral imaging.

Keywords: metamaterials, Ising model, terahertz, Fano

Longqing Cong, Vassili Savinov, Yogesh Kumar Srivastava, Song Han, and Ranjan Singh*

Metamaterial analogue of Ising model

TOC figure